Influence of Sulfur Metalation on the Accessibility of the $Ni^{II/I}$ Couple in [*N*,*N*′-Bis(2-mercaptoethyl)-1,5-diazacyclooctanato]nickel(II): Insight into the Redox Properties of [NiFe]-Hydrogenase

Ghezai Musie, Patrick J. Farmer,† Thawatchai Tuntulani, Joseph H. Reibenspies, and Marcetta Y. Darensbourg*

Department of Chemistry, Texas A&M University, College Station, Texas 77843

Received August 23, 1995⊗

A redox model study of [NiFe] hydrogenase has examined a series of five polymetallics based on the metalation of the dithiolate complex [1,5-bis(mercaptoethyl)-1,5-diazacyclooctane]Ni(II), **Ni-1**. Crystal structures of three polymetallics of the series have been reported earlier: **$[(Ni\text{-}1)_2Ni]Cl_2$**, **$[(Ni\text{-}1)_2FeCl_2]_2$**, and **$[(Ni\text{-}1)_3(ZnCl)_2]Cl_2$**. Two are described here: **$[(Ni\text{-}1)_2Pd]Cl_2\cdot 2H_2O$** crystallizes in the monoclinic system, space group $P2_1/c$ with cell constants $a = 12.212(4)$ Å, $b = 7.642(2)$ Å, $c = 16.625(3)$ Å, $\beta = 107.69(2)°$, $V = 1443.230(0)$ Å^3, $Z = 2$, $R = 0.051$, and $R_w = 0.056$. **$[(Ni\text{-}1)_2CoCl]PF_6$** crystallizes in the triclinic system, space group $P\bar{1}$, with cell constants $a = 8.14(2)$ Å , $b = 13.85(2)$ Å , $c = 15.67(2)$ Å, $\alpha = 113.59(10)°$, $\beta = 101.84(14)°$, $\gamma = 94.0(2)°$, $V = 1561.620(0)$Å^3, $Z = 2$, $R = 0.072$, and $R_w = 0.077$. In all **Ni-1** serves as a bidentate metallothiolate ligand with a "hinge" angle in the range 105−118° and Ni−M distances of 2.7− 3.7 Å. The most accessible redox event is shown by EPR and electrochemistry to reside in the N_2S_2Ni unit and is the $Ni^{II/I}$ couple. Charge neutralization of the thiolate sulfurs by metalation can (dependent on the interacting metal) stabilize the Ni^{I} state as efficiently as methylation forming a thioether. The implication of these results for the heterometallic active site of [NiFe]-hydrogenase as structured from *Desulfovibrio gigas* (Volbeda, A., et al. *Nature,* **1995**, *373*, 580), the generality of the Ni(μ-SR)$_2$M hinge structure, and a possible explanation for the unusual redox potentials are discussed.

Introduction

A chemically intriguing result of the recently reported X-ray crystal structure of [NiFe] hydrogenase isolated from *Desulfovibrio gigas* (under aerobic conditions) was the discovery of an unidentified second metal ion bridged into the NiS_4 site by thiolate sulfurs of cysteines 68 and 533 of the enzyme.[1] At a distance ca. 2.6−2.7 Å from the nickel center, this unexpected metal is further ligated by non-protein ligands as well as a third bridge ligand in an incompletely occupied site.[1] According to Volbeda *et al.*,[1] the X-ray scattering properties and elemental analysis are consistent with assignment of the second metal as iron, which subsequent work supports,[1b] and a likeness of the presumed active site is sketched in structure **A**. As presently modeled at a refinement level of 2.85 Å resolution, the coordination of the four cysteine sulfurs about nickel creates neither tetrahedral nor square planar geometry but rather appears to be an octahedron with cis-open sites, one partially filled by the bridge ligand, possibly hydride, or hydroxide.[1]

Whereas further refinement of structural data is impending, the current level inspires a renewed interest in heterobimetallic structures and their role in providing answers to some remarkable and unexplained physical properties of the [NiFe] hydrogenases, long attributed to the nickel site.[2] Included are (1) the growth and disappearance of unique EPR signals which track enzymatic activity in various redox levels (Ni^0 (the EPR silent and enzymatically active "Ni-R" state); Ni^{I} (EPR and enzymatically active "Ni-C"; Ni^{II} (EPR silent and enzymatically inactive, "Ni-silent"); and Ni^{III} (EPR active and enzymatically inactive, in two forms, "Ni-A" and "Ni-B"); (2) an unusual redox potential for the $Ni^{II/III}$ couple from −0.15 to −0.40 V vs NHE whereas typical coordination complexes show values of +0.50 to +1.50 V,[3a] and (3) an unprecedentedly small potential window (ca. 0.50 V) that apparently permits access to both the $Ni^{II/I}$ and $Ni^{II/III}$ couples. Whereas ligand environments may be found which mimic the individual *values* of $Ni^{II/I}$ *or* $Ni^{II/III}$ potentials,[3b] mononuclear nickel complexes in a single ligand set show a *difference* between these couples of typically 2 V.[4] For example, the sterically bulky tetrathiolate complex reported

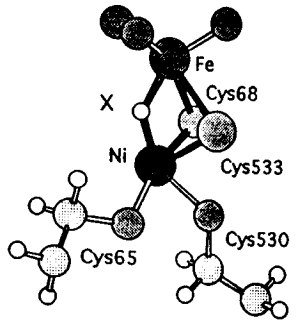

A

† Current address: Department of Chemistry, University of California, Irvine, Irvine, CA 92717.

⊗ Abstract published in *Advance ACS Abstracts,* March 15, 1996.

(1) (a) Volbeda, A.; Charon, M.-H.; Piras, C.; Hatchikian, E. C.; Frey, M.; Fontecilla-Camps, J. C. *Nature* **1995**, *373*, 580. (b) Volbeda, A.; Charon, M. -H.; Piras, C.; Hatchikian, E. C.; Frey, M.; Fontecilla-Camps, *J. Inorg. Biochem.* **1995**, *59*, 637.

(2) (a) Cammack, R.; Fernadez, V. M.; Schnieder, K. *The Bioinorganic Chemistry of Nickel*; Lancaster, J. R., Ed.; VCH Publishers: New York, 1988; Chapter 4 . (b) Cammack, R.; *Advances in Inorganic Chemistry*; Academic: New York, 1988; Vol. 32, p 297. (c) Halcrow, M. A.; Christou, G, *Chem. Rev.* **1994**, *94*, 2421. (d) Coremans, J. M. C. C.; Van der Zwaan, J. W.; Albracht, S. P. J. *Biochim. Biophys. Acta* **1989**, *997*, 256. (e) Adams, M. W. W.; Jin, S.-L. C.; Chen, J.-S.; Mortenson, L. E. *Biochim. Biophys. Acta* **1986**, *869*, 37. (f) Kovacs, J. A. *Adv. Inorg. Biochem.* **1993**, *9*, Chapter 5.

(3) (a) Krüger, H.-J.; Holm, R. H. *Inorg. Chem.* **1989**, *28*, 1148 and references therein. (b) Krüger, H.-J.; Peng. G.; Holm, R. H. *Inorg. Chem.* **1991**, *30*, 742.

(4) (a) Lovecchio, F. V.; Gore, E. S.; Busch, D. H. *J. Am. Chem. Soc.* **1974**, *96*, 3109. (b) Busch, D. H. *Acc. Chem. Res.* **1978**, *11*, 392.

0020-1669/96/1335-2176$12.00/0

Scheme 1

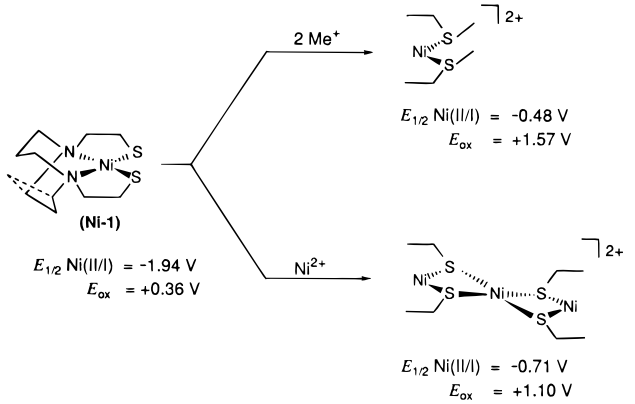

by Millar and co-workers produces a reversible $Ni^{III/II}$ couple (−0.52 V vs NHE) which closely matches that of the enzyme; however, this planar $Ni(SR)_4^{2-}$ complex cannot reasonably access Ni^{I}.[5]

An analysis of the redox properties of model complexes in light of the Volbeda, *et al*. structure surmised that "The structure determination of the binuclear NiM center raises as many questions as it answers."[6] Although more informative results arising from additional crystallizations and structural characterizations of the enzyme in various states of activation are expected, we are compelled to explore results of solution studies of model complexes with regard to the influence of a second metal site on the characteristics of nickel ions in sulfur ligation.

Previous work in our laboratories used the N_2S_2 title complex, **Ni-1**, to examine the effects of thiolate sulfur modification (alkylation, H-bonding, metalation, and oxygenation) on the redox properties of nickel, Scheme 1.[7] All such thiolate sulfur charge neutralization resulted in easing the accessibility of the reversible one-electron reduction couple (established by bulk reduction and EPR analysis to be $Ni^{II/I}$), with the opposite effect on the oxidation event (irreversible and complicated by S-based oxidation, or arising from a HOMO with considerable Ni−S character).[7] As reported in Scheme 1, this oxidative event is lowest for the dithiolate **Ni-1.** (Electrochemical conditions for the compounds in Scheme 1 are the same as in the caption of Figure 5.)

The gain of ca. 0.70 V per sulfur-site methylation placed the $Ni^{II/I}$ couple for the dicationic, dithioether (−0.48 V in CH_3CN (−0.46 V in H_2O) vs NHE) within the biological range. A similarly low potential observed for the trimetallic compound, **$(Ni\text{-}1)_2Ni^{2+}$**, led to the conclusion that sulfur metalation, generating a dicationic species, was analogous to methylation with respect to thiolate sulfur charge neutralization and the stabilization of Ni^{I}. That is, μ^2-bridging thiolates are metalated versions of thioethers.[7] Thus, the thiolate sulfur charge neutralization by S-metalation is a highly reasonable hypothesis to pursue in explanation of the observed low reduction potential of the enzyme. To this end and cognizant of the importance of the heterobimetallic [NiFe] site of hydrogenase, we have prepared a group of polynuclear complexes, using **Ni-1** as a metallothiolate ligand, and herein establish and interpret their redox characteristics. Several shown in Chart 1, including the important Ni−Fe tetrametallic complex **$[(Ni\text{-}1)FeCl_2]_2$**, were

Chart 1

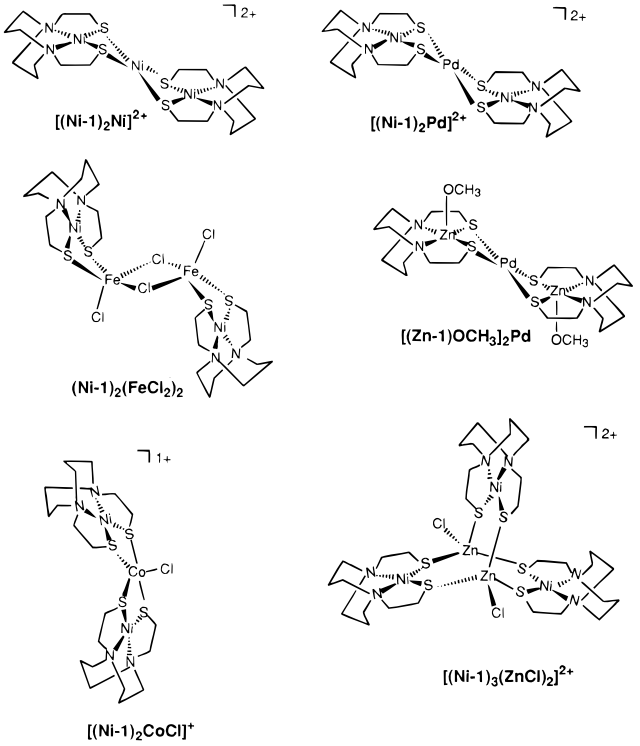

previously described.[8] The **$(Ni\text{-}1)_2Pd^{2+}$** and **$(Ni\text{-}1)_2CoCl^{+}$** are presented for the first time.

Since multiple redox events are possible in polymetallics, a trimetallic compound of zinc and palladium, **$[(Zn\text{-}1)(OMe)]_2Pd$** was used to establish the redox character of the central PdS_4 unit, in the absence of a second redox active metal. From this and EPR studies we will argue that the most accessible redox event in these metalated nickel thiolates is $Ni^{II/I}$ reduction, and that metalation can shift this couple by 1−1.5 V from its position in free **Ni-1**, dependent on the nature of the interacting metal. We will raise the issue of whether reversible metalation might account for (1) the narrow potential range encompassing $Ni^{II/I}$ or $Ni^{II/III}$ potentials in thiolate ligation, and (2) therefore the sentinel, if not the functional, properties of the nickel site in [NiFe]-hydrogenase.

Experimental Section

General Methods. Solvents were reagent grade and were purified according to published procedures.[9] Palladium dichloride was purchased from Strem Chemical Company and used as received. All other chemicals were purchased from Aldrich Chemical Co. and used as received. Where anaerobic techniques were required, an argon glovebox or standard Schlenk techniques were employed.

Physical Measurements. UV-vis spectra were recorded on a Hewlett-Packard HP8452A diode array spectrophotometer. Elemental analyses were performed by Galbraith Laboratories, Knoxville, TN.

All X-ray crystal structures were solved at the Crystal & Molecular Structure Laboratory Center for Chemical Characterization and Analysis at Texas A&M University. X-ray crystallographic data were obtained on a Siemens R3m/V single-crystal X-ray diffractometer operating at 55 kV and 30 mA, with Mo Kα ($\lambda = 0.71073$ Å) radiation, equipped with a Siemens LT-2 cryostat. Diffractometer control software P3VAX 3.42 was supplied by Siemens Analytical Instruments, Inc. All crystallographic calculations were performed with use of the Siemens

(5) Fox, S.; Wang, Y.; Silver, A.; Millar, M. *J. Am. Chem. Soc.* **1990**, *112*, 3218.
(6) Halcrow, M. A. *Angew. Chem., Int. Ed. Engl.* **1995**, *34*, 1193.
(7) Farmer, P. J.; Reibenspies, J. H.; Lindahl, P. A.; Darensbourg, M. Y. *J. Am. Chem. Soc.* **1993**, *115*, 4665.
(8) Mills, D. K.; Hsiao, Y. M.; Farmer, P. J.; Atnip, E. V.; Reibenspies, J. H.; Darensbourg, M. Y. *J. Am. Chem. Soc.* **1991**, *113*, 1421.
(9) Gordon, A. J.; Ford, R. A. *The Chemist's Companion*; Wiley and Sons: New York, 1972; pp 429−436.
(10) Sheldrick, G. *SHELXTL-PLUS Program for Crystal Structure Refinement*; Institüt für Anorganische Chemie der Universität: Gottingen, Germany, 1990.

Table 1. Summary of Crystallographic Data

	$[(Ni\text{-}1)_2Pd]Cl_2$	$[(Ni\text{-}1)_2CoCl](PF_6)$
chem formula	$C_{20}H_{44}N_4O_2S_4Cl_2PdNi_2$	$C_{20}H_{40}N_4F_6PS_4ClCoNi_2$
fw	795.6	821.6
space group	$P2_1/c$	$P\bar{1}$
a (Å)	12.212(4)	8.14(2)
b (Å)	7.462(2)	13.85(2)
c (Å)	16.625(3)	15.67(2)
V (Å^3)	1443.230(0)	1561.620(0)
α (deg)		113.59(10)
β (deg)	107.69(2)	101.84(14)
γ (deg)		94.0(2)
Z	2	2
temp (K)	193	296
R (R_w)[a] (%)	5.1 (5.6)	7.2 (7.7)

[a] Residuals defined: $R = \Sigma|F_o - F_c|/\Sigma F_o$; $R_w = \{[\Sigma w(F_o - F_c)^2]/[\Sigma w(F_o)^2]\}^{1/2}$.

SHELXTL-PLUS program package.[10] The structures were solved by direct methods. Anisotropic refinement for all non-hydrogen atoms was done by a full-matrix least-squares method. Cell parameter and data collection summaries for compounds **$[(Ni\text{-}1)_2Pd]Cl_2$** and **$[(Ni\text{-}1)_2CoCl]PF_6$** are given in Table 1.

EPR spectra were recorded on a Bruker ESP 300 equipped with an Oxford ER910A cryostat operating at 10 K. An NMR gaussmeter (Bruker ERO35M) and Hewlett Packard frequency counter (HP5352B) were used to calibrate the field and microwave frequency, respectively.

Conductance measurements were performed using an Orion Model 160 Conductance meter equipped with an Orion two-electrode conductivity cell. The cell constant was determined to be 0.112 cm^{-1}. The freshly distilled CH_3CN was found to have conductivity of 1.44 $\times$ 10^{-6} mhos.

Electrochemical measurements were performed using a Bioanalytical Systems 100A electrochemical analyzer equipped with three electrodes, using glassy carbon stationary electrode and platinum wire auxiliary electrode. Measurements in CH_3CN were 1.0−2.5 mM in analyte and 0.2 M in [*n*-Bu_4N](PF_6) (TBAHFP) as supporting electrolyte, and used a Vycor-tipped $Ag/AgNO_3$ reference electrode. All potentials were scaled to NHE using Cp_2Fe/Cp_2Fe^+ (the literature value for $E_{1/2}^{NHE}$ = 0.40 mV in acetonitrile)[11] as standard. All measurements were performed under N_2 atmosphere and room temperature except for **$(Ni\text{-}1)_2(FeCl_2)_2$** which was measured at 0 °C.

Syntheses. Complexes **Ni-1**,[12] **$(Ni\text{-}1)_2NiCl_2$**,[13] **$(Ni\text{-}1)_2(FeCl_2)_2$**,[8] and **$(Ni\text{-}1)_3(ZnCl_2)_2$**[14] were prepared according to published procedures.

$[(Ni\text{-}1)_2CoCl](PF_6)$. In a manner similar to the preparation of **$(Ni\text{-}1)_3(ZnCl_2)_2$**,[14] a methanolic solution (20 mL) of **Ni-1** (50 mg, 0.17 mmol) and $NaPF_6$ (30 mg, 0.18 mmol) was layered into a THF solution (15 mL) of $CoCl_2$ (15 mg, 0.12 mmol). The product, **$[(Ni\text{-}1)_2CoCl](PF_6)$**, crystallized from the solution as red crystals, ca. 40% yield. In the absence of $NaPF_6$ a red-brown powder was obtained and used for elemental analysis: **$[(Ni\text{-}1)_2CoCl]Cl\cdot 2H_2O$**: Anal. Calcd (found) for $C_{20}H_{44}Cl_2O_2N_4S_4Ni_2Co$: C, 32.22 (32.05); H, 5.95 (6.01). UV−vis in ethanol solution, λ_{max} (ϵ): 318 (138), and 528 (323) nm.

$[(Ni\text{-}1)_2Pd]Cl_2$. A 0.056 g portion of K_2PdCl_2 (0.5 equiv) was added to 0.100 g of **Ni-1** in 30 mL of CH_3CN, resulting in a color change from purple to deep red. Filtration and recrystallization by ether diffusion into the methanolic solution produced 91 mg (66% yield) of the dark purple crystalline dihydrate of **$[(Ni\text{-}1)_2Pd]Cl_2$** . UV−vis in ethanol: λ_{max} (ϵ): 408 (5245), and 522 (3730) nm. Anal. Calcd (found) for $C_{20}H_{44}N_4S_4O_2Ni_2Pd$: C, 30.17 (30.63); H, 5.53 (5.44).

Reduction of $[(Ni\text{-}1)_2Ni]Cl_2$. EPR Sample Preparation. To a 0.10 g (0.14 mmol) portion of the trimetallic compound dissolved in 30 mL of thoroughly degassed, distilled EtOH was added a 0.020 g (0.53 mmol) portion of $NaBH_4$, dissolved in 20 mL of EtOH. A color change from dark red-black to green was noted, and immediately a 0.50 mL sample was transferred to a 5 mm quartz tube, frozen at 77 K, and later cooled to 10 K for EPR analysis. A green-metallic solid product resulted from precipitation as the BPh_4^- salt. Attempts to crystallize the reduction product were unsuccessful. The other samples were similarly prepared. In addition to $NaBH_4$, cobaltocene and KHB[*sec*-Bu]$_3$ were used as reductants.

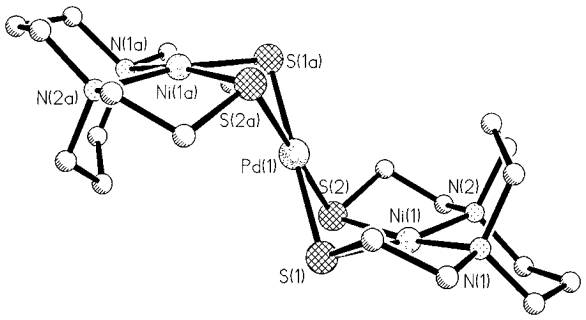

Figure 1. Molecular structure of **$[(Ni\text{-}1)_2Pd]^{2+}$**. The atoms labeled a are related by a crystallographic center of symmetry. Selected bond lengths (Å): Ni(1)−Pd(1), 2.823(2); Ni(1)−S(1), 2.176(2); Ni(1)−S(2), 2.170(3); Pd(1)−S(1), 2.297(2); Pd(1)−S(2), 2.293(2); Ni(1)−N(1), 1.962(7); Ni(1)−N(2), 1.951(6). Selected bond angles (deg): S(1)−Pd(1)−S(2), 79.9(1); S(1)−Pd(1)−S(2a), 100.1(1); S(1)−Ni(1)−S(2), 85.4(1); S(1)−Ni(1)−N(1), 91.4(2); S(2)−Ni(1)−N(2), 90.6(2); N(1)−Ni(1)−N(2), 91.3(3); Pd(1)−S(1)−Ni(1), 78.2(1); Pd(1)−S(2)−Ni(1), 78.4(1).

Results and Discussion

Molecular Structures. The group VIII trinuclear species **$[(Ni\text{-}1)_2Ni]X_2$** (X = Cl or Br) and **$[(Ni\text{-}1)_2Pd]Cl_2$** are isostructural, crystallizing in the monoclinic space group $P2_1/c$. Shown in Figure 1 is the step-like molecular structure of **$[(Ni\text{-}1)_2Pd]Cl_2$**, typical of such trimetallic compounds,[13] with the central Pd metal bridged by two thiolate sulfurs into the flanking **Ni-1** units. Pertinent metric data are listed in the figure caption, while a full report is available in the Supporting Information. The folding angle between the perfectly square planar PdS_4 and the best plane calculated for a NiN_2S_2 unit (mean deviations in the NiN_2S_2 planes are 0.0504 Å) is 108.9° whereas the analogous angle for the **$[(Ni\text{-}1)_2Ni]^{2+}$** unit is 103.4°. The greater folding angle and the larger Pd^{2+} ion size accounts for M−M separations in the heterotrimetallic compounds: Ni−Pd = 2.823(2) Å and Ni---Ni = 5.646 Å in **$[(Ni\text{-}1)_2Pd]Cl_2$**. In contrast the Ni(1)−Ni(2) distance in **$[(Ni\text{-}1)_2Ni]^{2+}$** is 2.685(1) and the Ni(1)---Ni(3) distance is 5.370 Å. These stepped structures are analogous to $[(H_2NCH_2CH_2S)_2Ni]_2Ni^{2+}$ whose Ni−Ni distance of 2.733 Å was cited as evidence of weak Ni−Ni bonding.[15]

The molecular structure of the Ni−Co heterometallic complex **$[(Ni\text{-}1)_2CoCl](PF_6)$** is shown in Figure 2, and an expanded view of the immediate coordination about the central Co^{II} is given in Figure 3. A search of >120 000 entries in the Cambridge Crystal Structure data base (CSD) found no Ni−Co bimetallic complexes with bridging thiolates.[16] As in the group VIII trimetallic compounds, two **Ni-1** metallothiolate ligands bind to Co^{II}, however in a different geometrical arrangement. Two thiolate sulfurs from each of the **Ni-1** units are in equatorial positions of a slightly distorted trigonal bipyramidal Co^{II} center. The remaining two thiolate sulfurs occupy the axial positions while the chloride ligand completes the trigonal plane. Thus

(11) Gagne, R. R.; Koval, C. A.; Lisensky, G. C. *Inorg. Chem.* **1980**, *19*, 2854.
(12) Mill, D. K.; Reibenspies, J. H.; Darensbourg, M. Y. *Inorg. Chem.* **1990**, *29*, 4364.
(13) Farmer, P. J.; Solouki, T.; Mills, D. K.; Soma,T.; Russell, D. H.; Reibenspies, J. H.; Darensbourg, M. Y. *J. Am. Chem. Soc.* **1992**, *114*, 4601.
(14) Tuntulani, T.; Reibenspies, J. H.; Farmer, P. J.; Darensbourg, M. Y. *Inorg. Chem.* **1992**, *31*, 3497.
(15) (a) Legg, J. I.; Neilson, D. O.; Smith, D. L.; Larsen, M. L. *J. Am. Chem. Soc.* **1968**, *90*, 5030 (b) Drew, M. G. B.; Rice, D. A.; Richards, K. M. *J. Chem. Soc., Dalton Trans.* **1980**, 2075.
(16) Allen, F. H.; Davies, J. E.; Galloy, J. J.; Johnson, O.; Kennard, O.; Macrae, C. F.; Mitchell, E. M.; Mitchell, G. F.; Smith, J. M.; Watson, D. G. J. *Chem. Inf. Comput. Sci.* **1991**, *31*, 187.

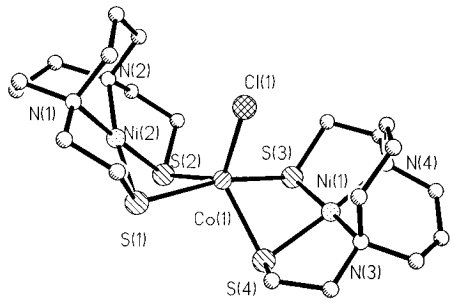

Figure 2. Molecular structure of **[(Ni-1)$_2$CoCl]**$^+$. Selected bond lengths (Å): Ni(1)−Co(1), 2.986 (9); Ni(1)−S(3), 2.159 (8); Ni(1)−S(4), 2.170 (8); Ni(1)−N(3), 1.96 (2); Ni(1)−N(4), 1.96(2). Selected bond angles (deg): S(3)−Ni(1)−S(4), 86.1(3); S(3)−Ni(1)−S(4), 75.0(2); S(3)−Ni(1)−N(4), 91.1(5); S(4)−Ni(1)−N(3), 90.6(5); N(3)−Ni(1)−N(4), 91.6(7); S(1)−Ni(2)−S(2), 85.8(2); S(1)−Ni(2)−N(1), 91.7(4); S(2)−Ni(2)−N(2), 91.4(4); N(1)−Ni(2)−N(2), 90.8(5). The caption of Figure 3 lists Co−S and Co−Cl bond parameters.

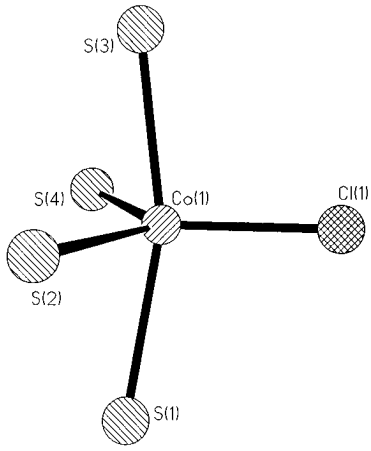

Figure 3. Distorted trigonal bipyramid coordination of the Co(II) center of **[(Ni-1)$_2$CoCl]**$^+$. Bond distances (Å): Co(1)−S(1), 2.488(8); Co(1)−S(2), 2.353(9); Co(1)−S(3), 2.467(8); Co(1)−S(4), 2.385(9); Co(1)−Cl(1), 2.296(8). Bond angles (deg): S(2)−Co(1)−S(4), 117.0(3); Cl(1)−Co(1)−S(2), 121.9(3); Cl(1)−Co(1)−S(4), 121.1(3); S(1)−Co(1)−S(3), 163.2(3); Cl(1)−Co(1)−S(3), 98.1(2); S(2)−Co(1)−S(3), 94.6(2); S(3)−Co(1)−S(4), 75.0(2); Cl(1)−Co(1)−S(1), 98.6(2); S(1)−Co(1)−S(4), 98.0(2); S(1)−Co(1)−S(2), 74.7(2).

the preference of Co^{II} for tbp geometry induces a twist in the two planar NiN_2S_2 units with respect to each other. In **[(Ni-1)$_2$CoCl]**$^+$ the angle between the normals of the best NiN_2S_2 planes is 93.7°, significantly different from that in **[(Ni-1)$_2$Pd]**$^{2+}$ or **[(Ni-1)$_2$Ni]**$^{2+}$ in which the two NiN_2S_2 planes are parallel. The normal of the trigonal plane of S_2ClCo^{II} is at an angle of 58.3 and 59.5° with the respective normals of the two N_2S_2 planes. There is a slight opening of the ∠S−Ni−S angle to 86° as compared to the stepped structure of **[(Ni-1)$_2$Ni]**$^{2+}$ where **Ni-1** is a bidentate ligand in a square plane. In that case, the ∠S−Ni−S angles average to 82.8°. In all polymetallics the Ni−N and Ni−S distances are largely unchanged from those in the free **Ni-1** molecule.

The **[(Ni-1)(FeCl$_2$)]$_2$** heterotetrametallic compound, whose structure is depicted in Chart 1, provides an interesting contrast to **[(Ni-1)$_2$CoCl]**$^+$. The pentacoordinate irons are in pseudo square pyramidal geometry with sulfurs of the metallothiolate ligand and two bridging chlorides in basal positions; the iron is 0.754 Å out of the S_2Cl_2 base toward the terminal chloride in axial position. The pentametallic **(Ni-1)$_3$(ZnCl)$_2$**$^{2+}$ is structurally dissimilar from the other members of the series as the **Ni-1** serves as a bidentate bridging ligand and the sulfurs are "exo"-metalated, resulting in an opening of the ∠S−Ni−S to 88.1° as compared to the analogous ∠S−Ni−S of 82−84° typically seen for the "endo"-metalates.[8] Table 2 compares metric data of the polymetallics.

Bulk Reduction of [(Ni-1)$_2$Ni]Cl$_2$. As described in the Experimental Section, reduction of the trimetallic compound with $^1/_3$ mol (based on the trimetallic compound) of cobaltocene, $NaBH_4$, or $KHB(sec\text{-}Bu)_3$ gives rise to green **[(Ni-1)$_2$Ni]**$^+$ which could be isolated as its BPh_4^- salt. On exposure to O_2, the green species reverts to red-black **[(Ni-1)$_2$Ni]**$^{2+}$. The EPR spectrum of presumably **[(Ni^I-1)(Ni^{II}-1)Ni^{II}]**$^+$ measured in frozen ethanol solution is shown in Figure 4 along with the very similar spectrum of the Ni^I complex (also green) prepared by reduction of the cationic dithioether **[Me$_2$-Ni-1]**$^{2+}$ shown in Scheme 1.[7] The axial ($g_{\|} > g_{\perp}$) signals seen for both are consistent with the N_2S_2 nickel reduction with the unpaired electron in the $d_{x^2-y^2}$ orbital; the *g* values are practically identical.[17]

Electrochemistry. Cyclic voltammograms in the cathodic potential region for **[(Ni-1)$_2$Ni]**$^{2+}$ and **[(Ni-1)$_2$Pd]**$^{2+}$ compounds are found in Figure 5 and for **[(Ni-1)$_3$(ZnCl)$_2$]** in Figure 6. In the latter case, the scan was reversed at different potentials in order to isolate successive reduction waves. The observed match of the number of reduction waves to the number of (N_2S_2-Ni) sites in the trimetallic compound and pentametallic complexes is corroborated by square wave (SW) voltammograms which amplify the separate electrochemical events, as well as establish the validity of SW voltammetry for enhancing interpretation of less obvious CV's. (N.B.: An irreversible anodic wave also exists for **[(Ni-1)$_2$Ni]**$^{2+}$ and **[(Ni-1)$_2$Pd]**$^{2+}$ at +1.10 and +0.58 V, respectively, *vide infra.)* There is no indication that the group VIII trimetallic compounds, in their original or reduced states, deaggregate in dry CH_3CN.

Since it is arguable that the redox activity of the trimetallic compounds **[(Ni-1)$_2$M]**$^{2+}$ (M = Ni, Pd) resides in the central MS_4 unit, we attempted to prepare a Zn/Ni heterometallic from reaction of dimeric **(Zn-1)$_2$** with $NiCl_2$.[14] Unfortunately, Ni^{2+} displaced Zn^{2+} from the N_2S_2 coordination sphere. Thus the trimetallic compound containing a zinc dithiolate, **[(Zn-1)-OCH$_3$]**$^-$ as a redox inactive metallothiolate ligand to palladium(II) was prepared and characterized (X-ray crystal structure).[18] The structure of **[(Zn-1)(OCH$_3$)]$_2$Pd**, represented in Chart 1, shows a PdS_4 central unit similar to that of **[(Ni-1)$_2$Pd]**$^{2+}$. In the 0.00 to −1.60 V range this neutral complex shows no redox activity in methanol. The neutral **Pd-1** shows a Pd$^{II/I}$ reduction at −2.10 V,[19] while the dicationic **[Me$_2$-Pd-1]**$^{2+}$ is at ca. −1.0 V. We conclude that the PdS_4 unit is the less likely site of redox activity in **[(Ni-1)$_2$Pd]**$^{2+}$, and eq 1 best describes the reduction of the trimetallic. Although the NiS_4 site remains a possibility for the first electron reduction in the **[(Ni-1)$_2$Ni]**$^{2+}$ species, eq 2, the similarities and trends of electrochemical results within the series, as well as the similarity of the EPR spectra of reduced **[Me$_2$-Ni-1]**$^{2+}$ and reduced **[(Ni-1)$_2$Ni]**$^{2+}$, are taken as substantial evidence that the reduction waves seen in the series **[(Ni-1)$_2$Ni]**$^{2+}$, **[(Ni-1)$_2$Pd]**$^{2+}$, and **[(Ni-1)$_3$(ZnCl)$_2$]**$^{2+}$ are due to the N_2S_2Ni units. It should also be noted that the methylated or thioether derivatives, **[Me$_2$-Ni-1]**$^{2+}$ and **[Me-Ni-1]**$^+$, accept only one electron within the CH_3CN solvent potential

(17) Lappin, A. G.; Mc Auley, A. *Adv. Inorg. Chem.* **1988**, *32*, 241.
(18) Tuntulani, T. Ph.D. Dissertation, Texas A&M University, College Station, TX, 1995. X-ray diffraction data were collected at 23 °C on a Siemens R3m/v diffractometer. Structure was solved by standard procedures; empirical absorption corrections were applied. Crystallographic data are given as *a, b, c;* β, space group, *Z*, 2Θ range, unique observed reflections, *R* (R_w) (%). **[(Zn-1)$_2$(OCH$_3$)$_2$Pd]**: 9.053(10), 14.070(2), 12.731(10) Å; 94.48(10)°, $P2_1/c$, 2, 5.0/120°, 1955 ($I > 2\sigma(I)$), 3.1 (3.7). Structure deposited in Z. für Kristallogr., in press.
(19) Tuntulani, T.; Musie, G.; Reibenspies, J. H.; Darensbourg, M. Y. *Inorg. Chem.*, in press.

Table 2. Selected Metric Data for Polymetallic Derivatives of **Ni-1**

complex	[Ni]−M_{av}[a] (Å)	[Ni]−[Ni] (Å)	M−S_{av} (Å)	Ni−S (Å)	ref
Ni-1				2.159(3)	12
[(Ni-1)$_2$Ni]$^{2+}$	2.685(1)	5.370	2.199(1)	2.152(1)	13
[(Ni-1)$_2$Pd]$^{2+}$	2.823(2)	5.646	2.295(2)	2.173(2)	this work
[(Ni-1)$_2$CoCl]$^{+}$	2.982(9)	5.958	2.424(8)	2.165(8)	this work
(Ni-1)$_2$ ($FeCl_2$)$_2$	3.100(1)	8.140	2.552(3) 2.462(3)	2.169 (2)	8
[(Ni-1)$_3$($ZnCl_2$)$_2$]$^{2+}$	3.665(1)	5.110	2.361(5)	2.186(5)	14

[a] Where [Ni] is the nickel in the **Ni-1** unit and M is the metalating ion.

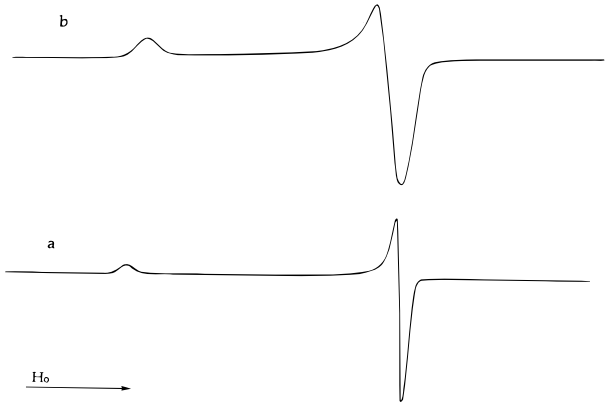

Figure 4. X-band EPR spectra obtained from ethanol solutions of (a) **[(Ni-1)$_2$Ni]Cl$_2$**, ($g_\perp$ = 2.05 and $g_\parallel$ = 2.23), and (b) **Me$_2$(Ni-1)Cl$_2$** ($g_\perp$ = 2.07 and $g_\parallel$ = 2.24) after reaction with 1 equiv of KBH(*sec*-Bu)$_3$. All spectra obtained at 10 K.

window.[20] Thus the evidence suggests that the first step in the reduction of the trimetallic compounds results in a Ni^I dithiolate stabilized by an M^{II} ion interacting at sulfur. The interpretation of the second reduction step is less straight forward; hence the 2-electron reduced species expressed in eqs 1 and 2 are strictly speculatory.

$$[(Ni^{II}\text{-}1)M^{II}(Ni^{II}\text{-}1)]^{2+} \overset{e^-}{\rightleftharpoons} [(Ni^{I}\text{-}1)M^{II}(Ni^{II}\text{-}1)]^{+} \overset{e^-}{\rightleftharpoons} [(Ni^{I}\text{-}1)M^{II}(Ni^{I}\text{-}1)] \quad (1)$$

$$[(Ni^{II}\text{-}1)M^{II}(N^{II}\text{-}1)]^{2+} \overset{e^-}{\rightleftharpoons} [(Ni^{II}\text{-}1)M^{I}(Ni^{II}\text{-}1)]^{+} \overset{e^-}{\rightleftharpoons} [(Ni^{I}\text{-}1)M^{I}(Ni^{II}\text{-}1)] \quad (2)$$

Figure 8 shows the cyclic and square wave voltammograms of **[(Ni-1)$_2$CoCl]Cl**. The CV features of the **[(Ni-1)$_2$CoCl]Cl**, are similar to those of the trinuclear species, **[(Ni-1)$_2$Ni]Cl$_2$** and **[(Ni-1)$_2$Pd]Cl$_2$**. The first reduction wave of **[(Ni-1)$_2$CoCl]Cl**, is reversible and occurs at −0.88 V; the second at −1.77 V is irreversible and ill-defined compared to the other trimetallic compounds.

The low solubility and structural instability of the tetranuclear **(Ni-1)$_2$(FeCl$_2$)$_2$** complex produced a poor quality cyclic voltammogram. The electrochemistry was performed at 0 °C to minimize degradation. Nevertheless, as shown in Figure 7, the square wave voltammograms showed evidence of the $FeCl_2$ and **Ni-1** components at −0.19 and −1.94 V, respectively (verified by "spiking" with pure compounds). Conductivity measurements of **(Ni-1)$_2$(FeCl$_2$)$_2$** in CH_3CN solution gave Λ ($cm^2\ mol^{-1}\ ohm^{-1}$) of 172−90 over the concentration range of 1.44−5.60 ($\times 10^6$ M), suggesting at least a 1:1 electrolyte, or possibly a mixture of 1:1 and 2:1 electrolytes.[21] Accordingly, the remaining reduction events at −0.64 and −1.53 V are assigned to iron-bound **Ni-1** units as indicated in Scheme 2. The more accessible reduction is expected to result from one of the Ni^{II} cationic species derived from chloride dissociation; the dicationic species would be most analogous to the **[Me$_2$-Ni-1]$^{2+}$** reduction, *vide infra*.

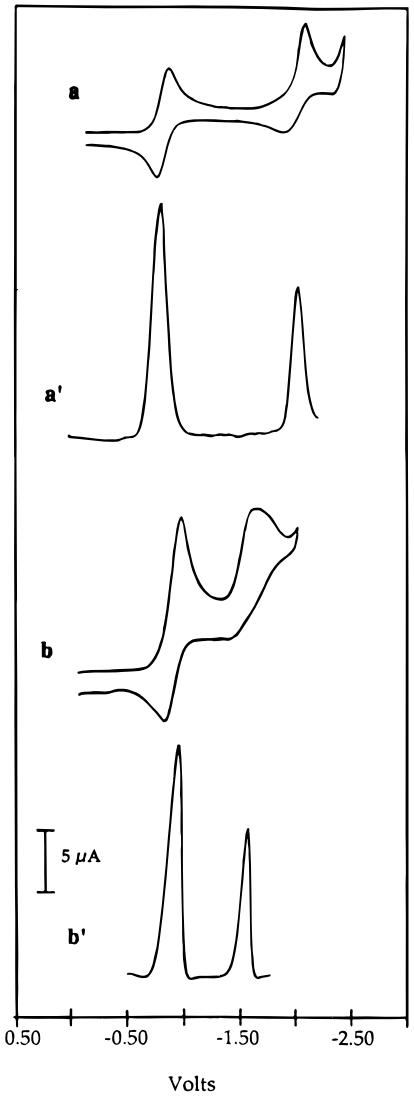

Figure 5. Cyclic voltammograms of 2.5 mM solutions of (a) **[(Ni-1)$_2$Ni]Cl$_2$** and (b) **[(Ni-1)$_2$Pd]Cl$_2$** in 0.1 mM TBAHFP/CH_3CN with a glassy carbon electrode at a scan rate of 200 mV/s. Scans of the square-wave voltammograms **a′** and **b′** are initiated in the negative direction; square-wave voltammogram amplitude = 25 mV; frequency = 15 Hz; E_{step} = 4 mV. All potentials are scaled to NHE.

A tabulation of the reduction potentials for the polymetallics is found in Table 3, and compared to the free **Ni-1** dithiolate and methylated or thioether derivatives, **[Me$_2$-Ni-1]$^{2+}$** and **[Me-Ni-1]$^{+}$**. The effect of metalation, and the development of a positive charge, substantially shifts the $Ni^{II/I}$ reduction potential to more positive values as compared to the free **Ni-1** dithiolate.

(20) Farmer, P. J. Ph.D. Dissertation, Texas A&M University, College Station, TX, USA. 1994.

(21) (a) Geary, W. J. *Coord. Chem. Rev.* **1971**, *7*, 81. (b) Borman, C.; Darensbourg, M. Y. *Inorg. Chem.* **1976**, *15*, 3121.

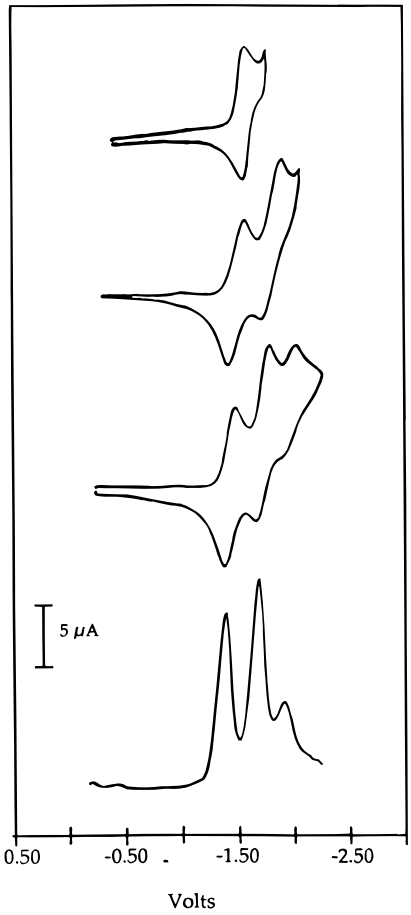

Figure 6. Cyclic voltammograms (with scan reversals to isolate successive waves) of 2.5 mM solutions of **[(Ni-1)$_3$(ZnCl)$_2$]Cl$_2$** in 0.1 mM TBAHFP/CH_3CN with a glassy carbon working electrode at 200 mV/s scan rate. Conditions for the square wave voltammogram are given in the caption of Figure 4.

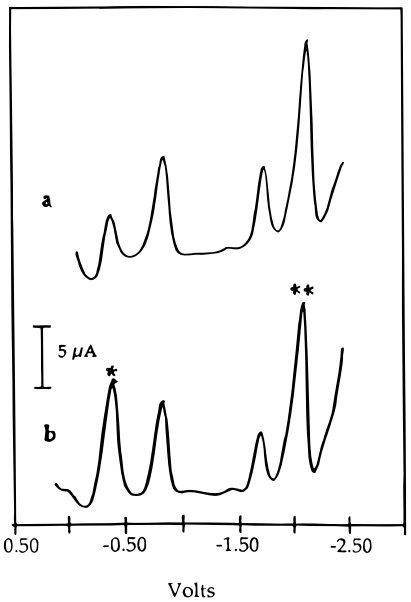

Figure 7. Square-wave voltammograms: of a 1.5 mM solution of (a) **(Ni-1)$_2$(FeCl$_2$)$_2$** in TBAHFP/CH_3CN at 0 °C; (b) after successive additions of $FeCl_2 \cdot 4H_2O$ (*) and **Ni-1** (**) to the solution.

The electronic character of the resulting sulfur donor is thus analogous to the thioether formed by alkylation, but the effect of metalated or μ-thiolate donors may be complicated by factors such as variable charge, metal−metal interactions, and different orientations of the Ni−S−M bridge. For example, the exo-

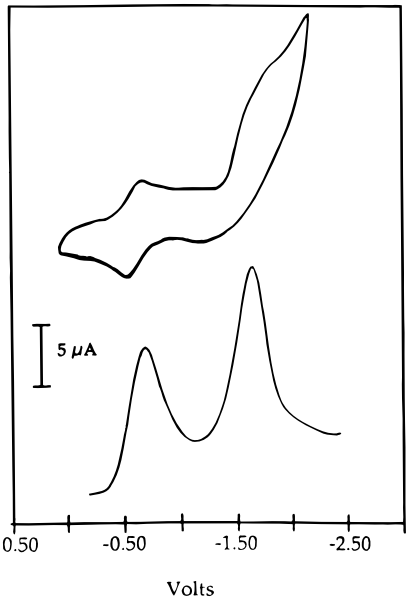

Figure 8. Cyclic and square-wave voltammograms of 1.5 mM solutions of **[(Ni-1)$_2$CoCl]Cl** in 0.1 mM TBAHFP/CH_3CN with a glassy carbon working electrode at 200 mV/s scan rate. Conditions for the square wave voltammograms are in the caption of Figure 4.

Scheme 2

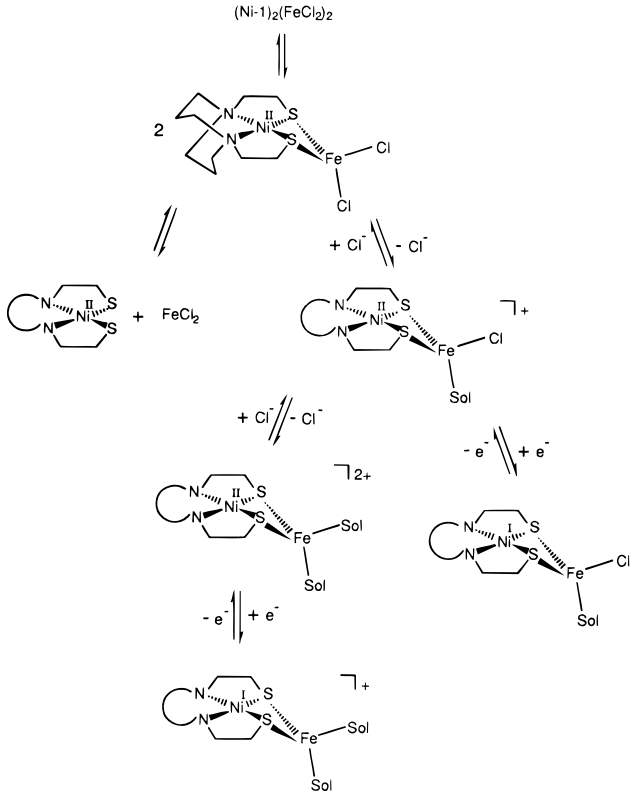

metalated derivative, **(Ni-1)$_3$(ZnCl)$_2^{2+}$**, produces the smallest effect, accountable to the smaller charge/size ratio of the intact pentanuclear species, as well as the exo-metalation of *cis*-thiolate sulfurs, and the fact that two unipositive cations, $ZnCl^+$, interact with three nickel dithiolates. In the case of the trimetallic compounds, especially **[(Ni-1)$_2$Ni]$^{2+}$** and **[(Ni-1)$_2$Pd]$^{2+}$**, the second metal, almost within bonding distance of the nickel, not only is expected to not only neutralize the charge of thiolate sulfur but also has the possibility to couple with other N_2S_2Ni units and delocalize the added electron. This charge delocalization should affect the potential for the second added electron more than the first, and is further explored below in this context.

Table 3. Comparison of $Ni^{II/I}$ Reduction Potential for S-Metalates of **Ni-1**

complex	$E_{1/2}Ni^{II/I}$ [V]	E_{pc} [V]	ΔE^b [V]
(Ni-1)	−1.94[13]		
[Me(Ni-1)]Cl	−1.20[13]		
[Me_2(Ni-1)]Cl_2	−0.48[13]		
[(Ni-1)$_2$ ($FeCl_2$)$_2$]^c	−0.64	−1.53	
[(Ni-1)$_2$Ni]Cl_2	−0.71	−1.66	0.95
[(Ni-1)$_2$Pd]Cl_2	−0.82	−1.36	0.54
[(Ni-1)$_2$CoCl]Cl	−0.88	−1.77	0.89
[(Ni-1)$_3$(ZnCl)]Cl_2	−1.08, −1.30, −1.50		0.22, 0.20[d]

[a] All potentials scaled to NHE referenced to a Cp_2Fe^+/Cp_2Fe standard ($E_{1/2}$ = 0.40 mV). In CH_3CN solutions, 0.1 M TBAHFP electrolyte, measured vs $Ag/AgNO_3$ reference electrode. [b] Difference between the first and the second reduction. [c] The measurement is taken at 0 °C. [d] The potential differences refer to the consecutive reduction events.

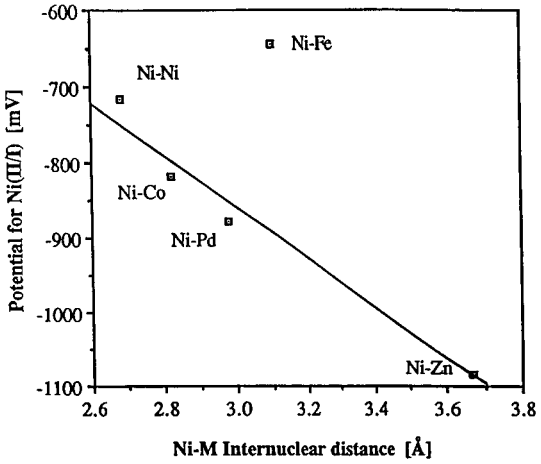

Figure 9. Plot of $E_{1/2}$, of the first reduction wave of the polymetallics vs the Ni−M internuclear distance.

Various metric parameters in Table 2 might be compared to the electrochemical data of Table 3. Four members of the series show a linear inverse correlation between the $Ni-M^{2+}$ distance and the most positive $Ni^{II/I}$ couple in each case, Figure 9. Off the line of Figure 9 is Ni-Fe, with a larger-than-expected $E_{1/2}$ value for the Ni-M distance. As discussed above, since the **(Ni-1)$_2$($FeCl_2$)$_2$** complex yields the $Ni^{II/I}$ couple closest to the **[Me_2-Ni-1]$^{2+}$**, deaggregation and ionization to yield a cationic species best accounts for the similarity. [The difference in temperature (the Ni-Fe complex was studied at 0 °C whereas all others were at ca. 22 °C) is expected to have a minor effect on potential.][22]

Electron Delocalization. Whereas the multiple cathodic events of the **(Ni-1)$_2$ ($FeCl_2$)$_2$** species are accountable to electron uptake by fragments and partially ionized species, the correspondence of the cathodic waves in the more stable **[(Ni-1)$_2$M]$^{2+}$** and the pentametallic **[(Ni-1)$_3$($ZnCl)_2$]$^{2+}$** to the number of **Ni-1** units suggest successive reductions of Ni^{II} to Ni^{I} in individual **Ni-1** units. For these intact polymetallics, the difference between the first and the second reductions (or, in the case of **[(Ni-1)$_3$($ZnCl)_2$]$^{2+}$**, first, second and third events) is taken as the measure of the delocalization and stability of the mixed valence species formed on initial reduction of the complex. For example, in **[(Ni-1)$_2$M]$^{2+}$** such delocalization would be expressed by the following resonance forms: $Ni^{I}-M^{II}-Ni^{II} \leftrightarrow Ni^{II}-M^{II}-Ni^{I}$. For the stable polymetallics the ΔE arguments put forth by Taube and co-workers for binuclear mixed valence ions of the form $(NH_3)Ru^{III}S\text{--}SRu^{II}(NH_3)_5$ (where S--S signifies a bridging dithioether ligand) are applicable.[23] If the central (or metalating) metal is Ni in the stepped **[(Ni-1)$_2$Ni]$^{2+}$** structure the delocalization, indicated by the magnitude of ΔE as listed in Table 3, is bigger than any member of the group. The larger Pd^{2+} and the presumed poorer energetic match of 3d vs 4d orbitals places the two Ni^{2+} ions in less communication in **[(Ni-1)$_2$Pd]$^{2+}$**. In the pentanuclear **(Ni-1)$_3$($ZnCl)_2^{2+}$**, the difference between the reduction waves of 0.20 V signifies substantial localization, as compared to **[(Ni-1)$_2$Ni]$^{2+}$** and **[(Ni-1)$_2$Pd]$^{2+}$**. This is consistent with both the nonoptimal geometry (for electronic delocalization) and the fact that the zinc is a d^{10} ion. Since the second reduction event in the **[(Ni-1)$_2$CoCl]Cl** complex is very ill-defined, further interpretation is little warranted. If, however, the species is intact and the second reduction results in the formation of two Ni^{I} species, charge delocalization is implied by the value of ΔE near to that of the **[(Ni-1)$_2$Ni]$^{2+}$** species. Further conclusions of the electron delocalization await studies of 61-Ni isotope specific site labeling by the Ni-61 isotope; such studies are underway.

Conclusions and Comments

The following are relevant to the structure/function of nickel in [NiFe]-hydrogenase.

(A) Throughout a series of five polymetallics the bidentate ligating properties of the metallodithiolato ligand **Ni-1** consistently generate "stair-case" or hinged structures with a possibility of Ni--M interaction due to a folding angle in the range of 104−118°. This angle is imposed by the optimization of S-lone pair orientation and geometrical requirement of the metal binding to the NiS_2 unit. This generality appears to hold for metalation of the *cis*-dithiolate of the NiS_4 unit in the active site of [NiFe]-hydrogenase.

(B) Whereas the free nickel(II) dithiolate complex **Ni-1** can undergo oxidation relatively easily, it cannot mimic, either in value or in product, the conversion from the EPR silent Ni^{II} state to the catalytically inactive Ni-A or Ni-B which, based on EPR results, contains Ni^{III}. As exemplified by Millar's $Ni(SR)_4^{2-}$ complex,[5] more thiolato-S donors (and a dianionic charge[4]) are required to bring the oxidation potential into biological range, while a sterically encumbered environment prevents S-oxidation and disulfide formation. Nevertheless our N_2S_2 complex is appropriate to examine for factors which might bring the $Ni^{II/I}$ reduction potential into range (i.e., the enzyme's easy conversion from the Ni^{II} state to the enzymically active "Ni-C" or Ni^{I} reduced form). This occurs when the thiolate sulfurs are charge neutralized, and we have found that S-site metalation is sufficient to change the donor ability of a thiolato-S to that of a thioether sulfur.[7] The reduction potential most like the previously studied dithioether **[Me_2-Ni-1]$^{2+}$** derives from the NiFe heterometallic **(Ni-1)$_2$($FeCl_2$)$_2$**, a complex which demonstrates deaggregation and chloride dissociation in solution. Suggestions regarding the solution forms of this complex, which were summarized in Scheme 2, implied that redox potentials might also be moderated by ligand ionization at the second metal site.

(C) Despite the substantial evidence that the most accessible redox activity is due to $Ni^{II/I}$ at the NiN_2S_2 site across the series of heteropolymetallic complexes in Scheme 1, there is still question as to the viability of the central NiS_4 as acceptor of the first electron in **[(Ni-1)$_2$Ni]$^{2+}$**. Thus argument may be made that the dimetalation of such as $Ni(SR)_4^{2-}$ unit, modeled by eq 3, leads to a tetrathioether type environment about the central Ni, which stabilizes Ni^{I} more so than the diamine-dithioether environment. Both possibilities however are consistent with a major role for S-metalation in mediating $Ni^{II/I}$ redox acitivity.

(22) Kadish, K. M.; Das, K.; Schaeper, D.; Merrill, C.; Welch, B. R.; Wilson, L. J. *Inorg. Chem.* **1980**, *19*, 2816.
(23) (a) Taube, H. Angew. *Chem., Int. Ed. Engl.* **1984**, *23*, 329. (b) Richardson, H. E.; Taube, H. *Inorg. Chem.* **1981**, *20*, 1278.

Scheme 3

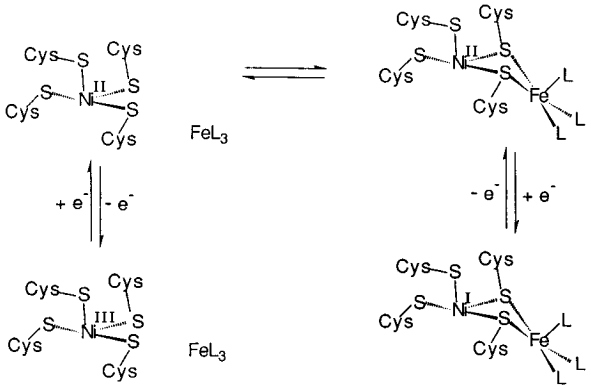

Other thiolate charge neutralization events such as methylation are less likely for the [NiFe]-hydrogenase, however protonation of one or more thiolates could also be operative.

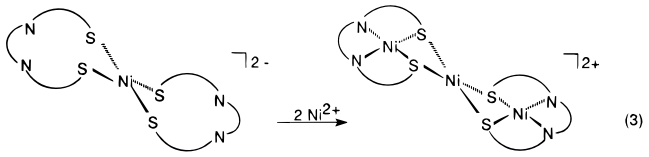

(D) To our knowledge, prior to this there were no electrochemical studies of the few reported thiolate-bridged Ni/Fe heterobimetallics.[24] An interesting interpretation of the various solution species of **(Ni-1)$_2$(FeCl$_2$)$_2$** is as prescient of an important feature in a new model for [NiFe]-hydrogenase. Scheme 3 expresses the possibility of a mobile FeL_3 unit whose on/off interaction with sulfur of nickel cysteinates, rationalizes the accessibility of Ni^I/Ni^{III}, respectively.[25] While attractive and consistent with the electrochemistry, this model leads to the conclusion that the oxidized state(s) (Ni-A and Ni-B) would be derived from a mononuclear, thiolate sulfur-rich nickel center, and the Ni(II) silent and Ni-C reduced states from the thiolate sulfur charge neutralized heterobimetallic. At this point the isolated and crystallized enzyme is in a mixture of states,[1b] and contains at least some enzyme which *should be* in the Ni-A or Ni-B oxidized states (or non-metalated).

Chart 2

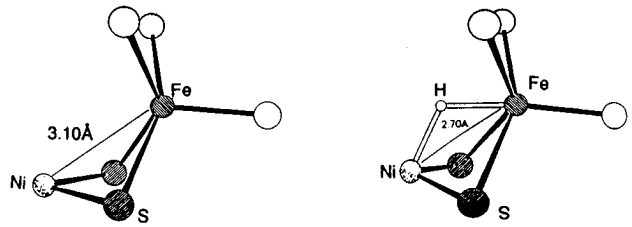

(E) The logic of Scheme 3, as well as the promise of more definitive and assuring structural characterizations of the enzyme when isolated in various states, inspires further examination as follows: The model complex **(Ni-1)$_2$(FeCl$_2$)$_2$**, which serves as structural/electrochemical precedent for Scheme 3, has an Ni−Fe distance of 3.1 Å, ca. 0.4 Å greater than that found in the heterobimetallic site of the *D. gigas* structure. Yet molecular modeling of a fragment, **(Ni-1)(FeCl$_2$)Cl**, found that on inserting a bridging hydride, forming Ni−H−Fe, the metals were drawn together (Chart 2) to a distance of 2.7 Å, comparable, if not in fact identical to, that found in the *D. gigas* hydrogenase structure,[1] and consistent with the suggestion[1] that the partially occupied bridging ligand could be hydride:

Thus a question arises in references to the likelihood and the source of a hydride in the *oxidized* form of the enzyme. Certainly there are examples of air-stable hydrides, especially when stabilized in a bridging environment.[27] Hence, the prospects of a Ni^{III}−H−Fe state, derived by protonation of a bimetallic Ni−C (Ni^I) as expressed above, or by heterolytic cleavage of H_2 from a $Ni^{III}\cdots\eta^2H_2$·Fe interaction are also worthy modeling problems.

(F) The long-standing proposition that nickel is merely a sentinel for the catalytic chemistry which might feasibly occur at a different site remains debatable. Focus can shift, however, from the FeS clusters to the mobile **FeL$_3$** fragment, its spin state, the possibilities for L,[28] and the regulatory mechanism whereby the unit might be moved into position sufficiently close for the S-metalation.

Acknowledgment. Financial support from the National Science Foundation (CHE 94-15901) for this work and CHE-8513273 for the X-ray diffractometer and crystallographic computing system, and contributions from the R. A. Welch Foundation are gratefully acknowledged. We thank Prof. Paul Lindahl for help with the EPR measurements and for sobering discussions.

Supporting Information Available: Tables of crystallographic data collection parameters, atomic coordinates and equivalent isotropic displacement parameters, complete bond lengths and bond angles, and anisotropic displacement parameters and packing diagrams for the complexes **[(Ni-1)$_2$Pd]Cl$_2$** and **[(Ni-1)$_2$CoCl](PF$_6$)** (11 pages). Ordering information is on any current masthead page.

IC9515968

(24) Colpas, G. J.; Day, R. O.; Maroney, M. J. *Inorg. Chem.* **1992**, *31*, 5053.
(25) In fact, EXAFS studies indicated a difference of ca. 0.30 Å in the Ni--Fe distances between the reduced and oxidized forms of the enzyme.[1b,26]
(26) Muller, A.; Erkens, A.; Schneider, K.; Muller, A.; Nolting, H.-F.; Henkel, G. *J. Inorg. Biochem.* **1995**, *59*, 643.
(27) Darensbourg, M. Y.; Walker, N.; Burch, R. R., Jr. *Inorg. Chem.* **1978**, *17*, 52.
(28) Bagley, A. K.; Van Gardner, C. J.; Chen M.; Duin, E. C.; Albracht, S. P. J.; Woodruf, W. H. *Biochemistry* **1994**, *33*, 9229.